Intramicroparticle nitrogen dioxide is a bubble nucleation site leading to decompression-induced neutrophil activation and vascular injury

Article *in* Journal of Applied Physiology: Respiratory, Environmental and Exercise Physiology · December 2012

DOI: 10.1152/japplphysiol.01386.2012 · Source: PubMed

6 authors, including:

Tatyana Milovanova
University of Pennsylvania
38 PUBLICATIONS **1,860** CITATIONS

SEE PROFILE

Donald Buerk
Drexel University
164 PUBLICATIONS **6,746** CITATIONS

SEE PROFILE

J Appl Physiol 114: 550–558, 2013.
First published December 20, 2012; doi:10.1152/japplphysiol.01386.2012.

Intramicroparticle nitrogen dioxide is a bubble nucleation site leading to decompression-induced neutrophil activation and vascular injury

Stephen R. Thom,[1,2] Ming Yang,[1] Veena M. Bhopale,[1] Tatyana N. Milovanova,[1] Marina Bogush,[1] and Donald G. Buerk[3]

[1]*Institute for Environmental Medicine and* [2]*Department of Emergency Medicine, University of Pennsylvania Medical Center, Philadelphia, Pennsylvania; and* [3]*School of Biomedical Engineering, Science and Health Systems, Drexel University, Philadelphia, Pennsylvania*

Submitted 16 November 2012; accepted in final form 19 December 2012

Thom SR, Yang M, Bhopale VM, Milovanova TN, Bogush M, Buerk DG. Intramicroparticle nitrogen dioxide is a bubble nucleation site leading to decompression-induced neutrophil activation and vascular injury. *J Appl Physiol* 114: 550–558, 2013. First published December 20, 2012; doi:10.1152/japplphysiol.01386.2012.—Inert gases diffuse into tissues in proportion to ambient pressure, and when pressure is reduced, gas efflux forms bubbles due to the presence of gas cavitation nuclei that are predicted based on theory but have never been characterized. Decompression stress triggers elevations in number and diameter of circulating annexin V-coated microparticles (MPs) derived from vascular cells. Here we show that ~10% MPs from wild-type (WT) but not inflammatory nitric oxide synthase-2 (iNOS) knockout (KO) mice increase in size when exposed to elevated air pressure ex vivo. This response is abrogated by a preceding exposure to hydrostatic pressure, demonstrating the presence of a preformed gas phase. These MPs have lower density than most particles, 10-fold enrichment in iNOS, and generate commensurately more reactive nitrogen species (RNS). Surprisingly, RNS only slowly diffuse from within MPs unless particles are subjected to osmotic stress or membrane cholesterol is removed. WT mice treated with iNOS inhibitor and KO mice exhibit less decompression-induced neutrophil activation and vascular leak. Contrary to injecting naïve mice with MPs from wild-type decompressed mice, injecting KO MPs triggers fewer proinflammatory events. We conclude that nitrogen dioxide is a nascent gas nucleation site synthesized in some MPs and is responsible for initiating postdecompression inflammatory injuries.

decompression sickness; intravascular bubble; leukocytes; platelets; antigen sharing; CD41; integrins; ultrasound

DECOMPRESSION SICKNESS (DCS) is a systemic pathophysiological process that occurs after tissues become supersaturated with gas. Inert gases inhaled while breathing are taken up by tissues in proportion to the ambient pressure, and when pressure is reduced, some of the gas released from tissues forms bubbles due to the presence of gas cavitation nuclei (7, 10, 42, 43). These nuclei have not been characterized. They are too small to be visually imaged or detected with ultrasound and their presence is discerned be showing they are eradicated with hydrostatic pressure (3, 20, 36). The central place of bubbles as an inciting factor for DCS is widely accepted, but the pathophysiological responses that mediate tissue injury remain unclear. DCS is a risk associated with deep sea diving, high-altitude aviation, and space exploration.

Address for reprint requests and other correspondence: S. R. Thom, Institute for Environmental Medicine, Univ. of Pennsylvania, 1 John Morgan Bldg., 3620 Hamilton Walk, Philadelphia, PA 19104-6068 (e-mail: sthom@mail.med.upenn.edu).

Decompression-induced elevations in circulating microparticles (MPs) occur in animals and humans after simulated or open-water SCUBA diving (18, 31, 37). MPs were shown to be responsible for inflammatory vascular injuries in a murine DCS model (32). MPs are defined as membrane lipid bilayer-enclosed vesicles with a diameter of 0.1–1.0 μm. MPs are present in peripheral blood of healthy individuals, increase with traumatic and inflammatory disorders, and may serve as intercellular messengers because they can contain cytokines or other signaling proteins, mRNA, and microRNA (19). MPs are generated when cells undergo oxidative stress, apoptosis, or cell activation/calcium influx, and they are characterized by surface expression of antigenic markers from parent cells (8, 9, 14, 25). As MPs bud from these cells, negatively charged phosphatidylserine residues are exposed, which often leads to secondary binding of annexin V. MPs can directly stimulate release of proinflammatory cytokines, and platelet-derived MPs stimulate leukocyte activation and aggregation (15, 17, 21). Annexin V-positive platelet-derived MPs exhibit procoagulant activity (2).

Recent studies have shown that some annexin V-positive particles enlarge beyond 1 μm in diameter during decompression (31, 32, 41). When injected into naïve mice, these large particles will recapitulate the pathophysiological vascular changes observed with provocative decompression (41). Particle size can be reduced by hydrostatic recompression, indicating that the enlarged particles contain a gas phase, and injecting these modified particles will not trigger the same inflammatory changes. One potential mechanism to explain this process is that some circulating particles normally have a gas nucleus so that on decompression, nitrogen from supersaturated tissues diffuses into the gas phase to cause particle enlargement. This is an appealing possibility because the size of the particles fits mathematical models of decompression pathophysiology that predict gas cavitation nuclei have a radius of up to ~0.6 μm (10, 42, 43). If indeed some MPs contain a gas phase in the normal state and prior to decompression, this represents a heretofore unknown characteristic that would add to the roles they play in pathophysiology and possibly in cell signaling. The goal of this investigation was to evaluate MPs and intraparticle gas.

METHODS AND MATERIALS

Materials. Unless otherwise noted, chemicals were purchased from Sigma-Aldrich (St. Louis, MO). Annexin binding buffer and the following antibodies were purchased from BD Pharmingen (San Jose, CA): fluorescein isothiocyanate (FITC)-conjugated anti-annexin V, FITC-conjugated anti-mouse myeloperoxidase (MPO), R-phycoerythrin (RPE)-conjugated anti-human CD142, PerCP/Cy5.5-conjugated anti-mouse CD41, PerCP/Cy5.5-conjugated anti-mouse CD14, allo-

phycocyanin (APC)-conjugated anti-mouse glycophorin A (Ter119, CD235), APC-conjugated anti-mouse CD31, and APC-conjugated anti-mouse vWF. R-PE-conjugated anti-mouse CD41 was purchased from e-Biosciences (San Diego, CA), PerCP Cy5.5-conjugated anti-human CD66b from Biolegend (San Diego, CA), and Alexa 647-conjugated anti-mouse CD18 from Serotec (Raleigh, NC).

Animals. All aspects of this study were reviewed and approved by the Institutional Animal Care and Use Committee (IACUC). Mice (*Mus musculis)* were purchased (Jackson Laboratories, Bar Harbor, ME), fed a standard rodent diet and water ad libitum, and housed in the animal facility of the University of Pennsylvania. A colony of iNOS KO mice, initially purchased from Jackson Laboratories, was maintained in the University vivarium. Mice were left to breathe room air (control) or subjected to 790 kPa (100 pounds per square inch) air pressure for 2 h following our published procedures (32, 41).

Standard procedures for MP acquisition and processing. All reagents and solutions used for MP analysis were sterile and filtered (0.2-μm filter). Heparinized blood was centrifuged for 5 min at 1,500 *g* and supernatant made 0.2 M EDTA to diminish ex vivo MP aggregation. This supernatant was centrifuged at 15,000 *g* for 30 min to pellet the few remaining platelets and cell debris. Supernatant was used in the ex vivo particle exposures to air pressure. Where indicated hydrostatic recompression was achieved by placing samples contained within closed plastic syringes inside a stainless steel pressure vessel that was pressurized to 790 kPa for 1 h as described previously (41).

Preparation of MPs from decompressed mice for reinjection into naïve mice followed our published protocol (41). Briefly, samples taken from the 15,000 *g* spin were parceled among centrifuge tubes at a ratio of 250 μl + 4 ml phosphate-buffered saline (PBS) and centrifuged at 100,000 *g* for 60 min (typically 3–4 tubes/experiment were used). Most fluid in the tubes was discarded and 250 μl remaining at the bottom used to resuspend the MP pellet. After MPs were counted to match numbers between wild-type and KO mouse samples, naïve mice were injected with MPs suspended in a total volume of 400 μl PBS via the tail vein. Endothelial leakage was evaluated 1 h after injection. Mice were anesthetized, exsanguinated, injected with lysine fixable Rhodamine-dextran (2×10^6 Da) and then with colloidal silica following published methods (32). Endothelium-enriched fractions were obtained for analysis from brain, leg skeletal muscle, psoas, and omentum.

For MP analysis on sucrose gradients, 500 μl MP supernatant from the 15,000 *g* spin was placed on a continuous linear sucrose gradient [2–87% (mass/vol), density = 1.006–1.320 g/ml]containing 0.02% sodium azide and 2 mM disodium EDTA and centrifuged at 158,000 *g* at 4°C for 18 h. After centrifugation all fractions were collected, and MPs counted and analyzed by flow cytometry.

To separate buoyant from denser MPs for biochemical analysis, 500 μl supernatant from the 15,000 *g* spin were combined with 4 ml PBS, centrifuged at 100,000 g for 60 min, the top 500 μl taken as the buoyant MPs sample, and the next 3.5 ml solution discarded, and the MP pellet was resuspended in the ~500 μl remaining in the centrifuge tube.

Flow cytometry. Flow cytometry was performed with a 10-color FACSCanto (Becton Dickinson, San Jose, CA) using standard acquisition software. Analysis of neutrophils and MPs was performed as previously described (32, 41).

Fluorescence probe studies. MPs isolated by ultracentrifugation and suspended in PBS were assayed in the presence of 5 μM 4,5-diaminofluorescein diacetate (DAF-DA), 10 μM 2,7-dihydrodichlorofluorescein diacetate (DCF-DA), or 5 μM DAF, and after 10 min, solutions were then made to 0.1% (vol/vol) PEG to lyse MPs and fluorescence monitored for 2–10 min longer. In some studies, solutions were prepared containing 100 μM PTIO [2-(4-carboxyphenyl)-4,5-dihydro-4,4,5,5-tetramethyl-1H-imidazolyl-1-oxy-3-oxide, monopotassium salt], a RNS scavenger, and in others when MPs were added the solution was 0.3 mM mannitol to cause an osmotic stress. In other studies, MPs obtained after the 15,000 *g* plasma centrifugation were incubated for 2 h at room temperature in a solution of 50 mM methyl–cyclodextrin (MCD), then diluted in PBS for centrifugation at 100,000 *g* for 60 min following the procedure described above. Where indicated MPs exposed to MCD for 2 h were isolated by ultracentrifugation and incubated overnight in a solution of 5 mM MCD containing 750 μM cholesterol before the fluorescence probe analysis. To inhibit NOS MPs were incubated for at least 30 min before fluorescence assays with up to 1 μM N-[[3-(aminomethyl)phenyl]methyl]-ethanimidamide, dihydrochloride) (1400W) or 10 mM L-N^G-nitroarginine methyl ester (L-NAME).

Nitrogen dioxide assay. The assay described by Wendel et al. (38) was used with some modifications. A 200 mM KOH solution containing 2 mM luminol was prepared and left in the dark at room temperature for at least 1 h before starting experiments. Assays were performed by adding 50 to 150 μl KOH/luminol to equal volumes of MPs at various concentrations suspended in PBS plus 10 mM EDTA. Some studies were performed in the presence of anti-oxidants/radical scavengers as follows: 2.5 mM Tiron, 1 mM ebselen [2-phenyl-1,2-benzisoselenazol-3(2H)-one], or 2.5 mM uric acid. In other studies MPs were incubated with 10 mM L-NAME for 1 h prior to the assay. Standards run on each day were performed with freshly prepared solutions of 3-morpholinosydnonimine (SIN-1) in PBS-EDTA, or by bubbling KOH/luminol with 500 ppm $^{\cdot}NO_2$ in air.

Microelectrodes. Microelectrodes selective for $^{\cdot}NO$ were fabricated and mounted in a hyperbaric chamber as described in previous studies (1, 30). Two-point calibrations for each electrode were made at 37°C in physiological buffer equilibrated with either 100% N_2 or 1,800 ppm $^{\cdot}NO$ (balance N_2). The electrodes were polarized at an oxidation potential of +850 mV relative to an Ag/AgCl reference electrode. Electrochemical oxidation currents were amplified with a sensitive electrometer (Keithley, model 610). The electrometer voltage output was low pass-filtered (analog circuit with 5-Hz cutoff) and digitized (1 sample/s) by computer. Current sensitivities ranged between 0.5 and 5 pA/μM. Electrodes were placed in 100 μl MP suspensions in microwell plates containing a small stir bar. After monitoring electrode readings for 30–60 min 0.7 μl of a 0.3% solution (wt/vol) of PEG was added and monitoring continued for an additional 60 min.

Confocal microscopy. Images of annexin V-positive particles were acquired using a Zeiss Meta510 confocal microscope equipped with a Plan-Apochromat 63×/1.4NA oil objective as previously described (32). Particle suspensions were stained with RPE-conjugated anti-annexin V antibody, combined with a small number of FITC-containing 0.86-μm beads (Sigma,) and placed on slides. Slides were first visually inspected to be sure no aggregates were present, then images were obtained and analyzed using ImageJ software.

Vascular permeability assay. Lysine-fixable tetramethylrhodamine-conjugated dextran (2×10^6 Da, Invitrogen, Carlsbad, CA) was prepared and used exactly as described in previous publications (32, 41). Vascular permeability, quantified as perivascular dextran uptake in experimental groups, was normalized to a value obtained with a control mouse included in each experiment.

Statistical analysis. We used Sigmastat software (Systat, Point Richmond, CA) for the statistical analysis. Neutrophil activation, elevations in size of different circulating annexin V-positive particle populations, and capillary leak were analyzed by ANOVA followed by the Holm-Sidak test. Single comparisons were performed using Student's *t*-tests.

RESULTS

MP enlargement with high air pressure. We hypothesized that if a portion of circulating MPs in normal, control air-breathing mice possess an intrinsic gas nucleation site they would enlarge on decompression following exposure to high gas pressure ex vivo. When particles from normal mice are surveyed only 2.6 ± 0.12% (mean ± SE, $n = 6$) of annexin

Table 1. *Microparticle diameters increase after particles isolated from mice were exposed to high air pressure for 22 h*

Particle Exposure	<1 μm Diameter	1–2 μm Diameter	>2 μm Diameter
WT			
Immediate fix	97.4 ± 0.13%	2.57 ± 0.12%	0.03 ± 0.02%
Ambient air	97.4 ± 0.11%	2.60 ± 0.11%	0.02 ± 0.02%
790 kPa air	91.3 ± 0.93%	6.00 ± 0.66%*	2.48 ± 0.15%*
HP then 790 kPa air	97.2 ± 0.17%	2.70 ± 0.18%	0.02 ± 0.03%
KO			
Immediate fix	97.3 ± 0.15%	2.70 ± 0.15%	0.00 ± 0.00%
Ambient air	97.7 ± 0.17%	2.33 ± 0.17%	0.00 ± 0.00%
790 kPa air	97.6 ± 0.14%	2.45 ± 0.14%	0.00 ± 0.00%
HP then 790 kPa air	97.5 ± 0.17%	2.48 ± 0.17%	0.00 ± 0.00%

Values are all means ± SE; $n = 6$. Data demonstrate the fraction of annexin V positive particles with diameters <1 μm, 1–2 μm, and >2 μm. Samples from wild-type (WT) or iNOS knockout (KO) mice were fixed immediately for measurements, or exposed to air at ambient pressure (101 kPa) or 790 kPa for 22 h, and where shown had been exposed for 1 h to 790 kPa hydrostatic pressure (HP) before the overnight air exposure. *Significantly different from others in same column ($P < 0.05$, ANOVA).

V-positive particles have diameters between 1 and 2 μm and 0.03 ± 0.02% are greater than 2 μm. As shown in Table 1, however, after being incubated with 790 kPa air pressure for 22 h, over 8% were found to have diameters exceeding 1 μm. If MPs are first subjected to 790-kPa hydrostatic pressure for 1 h before the overnight high pressure air exposure, which would eradicate a preformed gas phase, enlargement postdecompression did not occur.

Buoyancy of MPs. We reasoned that MPs containing a gas phase would be less dense that purely fluid-filled particles and this could be assessed by centrifugation through a sucrose gradient. Studies were conducted on normal, air-breathing mice and also 1 h after mice had been exposed to 790 kPa air pressure for 2 h, our standard animal model exposure (32, 41). As shown in Fig. 1, compared with controls the decompressed mice had a significantly higher proportion of MPs in the uppermost layer comprised mostly of PBS (labeled F0). There were no significant differences in the proportion of MPs found in other gradient layers with higher densities.

The standard way MPs are characterized is based on expression of proteins from parent cells on the membrane surface. We probed surface markers for neutrophils (CD66b), platelets (CD41a), endothelium (CD31 and vWF), all leukocytes (CD14), erythrocytes (CD235a, glycophorin A), and also tissue factor (CD142) as a potential pathological agent. Variations among layers are apparent in Fig. 2, but there were no significant differences in the proportion of each marker when comparing fractions between control and decompressed mice.

The ultracentrifugation technique used for obtaining MPs will also harvest exosomes, vesicles formed by invaginations of multivesicular bodies. Although exosomes are defined as smaller than MPs (50- to 100-nm diameter) with densities in the range of 1.15–1.19 g/ml in a sucrose gradient, if they possessed a gas phase their size and density may differ from the norm after decompression. Therefore, MP samples were probed for the endocytic marker Alix-1 and well as the tetraspanin CD63, as both are commonly found on exosomes (29). MPs from control and decompressed mice were prepared, placed in PBS, and subjected to ultracentrifugation to evaluate buoyant and pellet fractions. No significant differences were found. Buoyant control mouse samples ($n = 4$) exhibited 12.5 ± 8.2% CD63 and 16.5 ± 6.7% Alix-1, whereas decom-

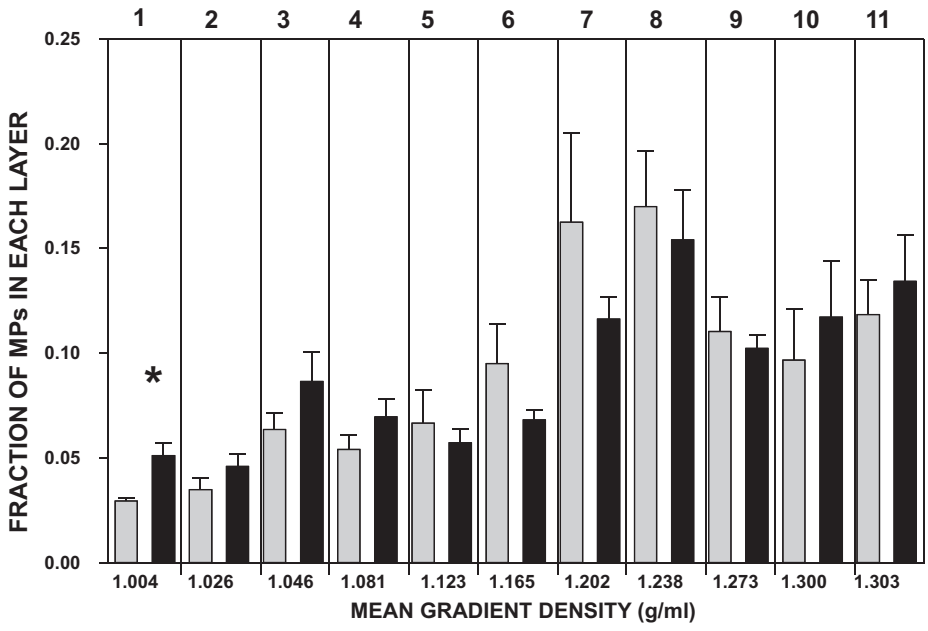

Fig. 1. Fraction of microparticles (MPs) found in various layers after sucrose gradient centrifugation of samples from air-breathing, control mice (gray bars), and those first subjected to decompression stress (black bars), which was a 2 h exposure to 790 kPa air followed by 1 h at ambient pressure. Mean gradient density is shown; variability across multiple experiments was <5%. Values are means ± SE; $n = 4$ in each group. *$P < 0.05$.

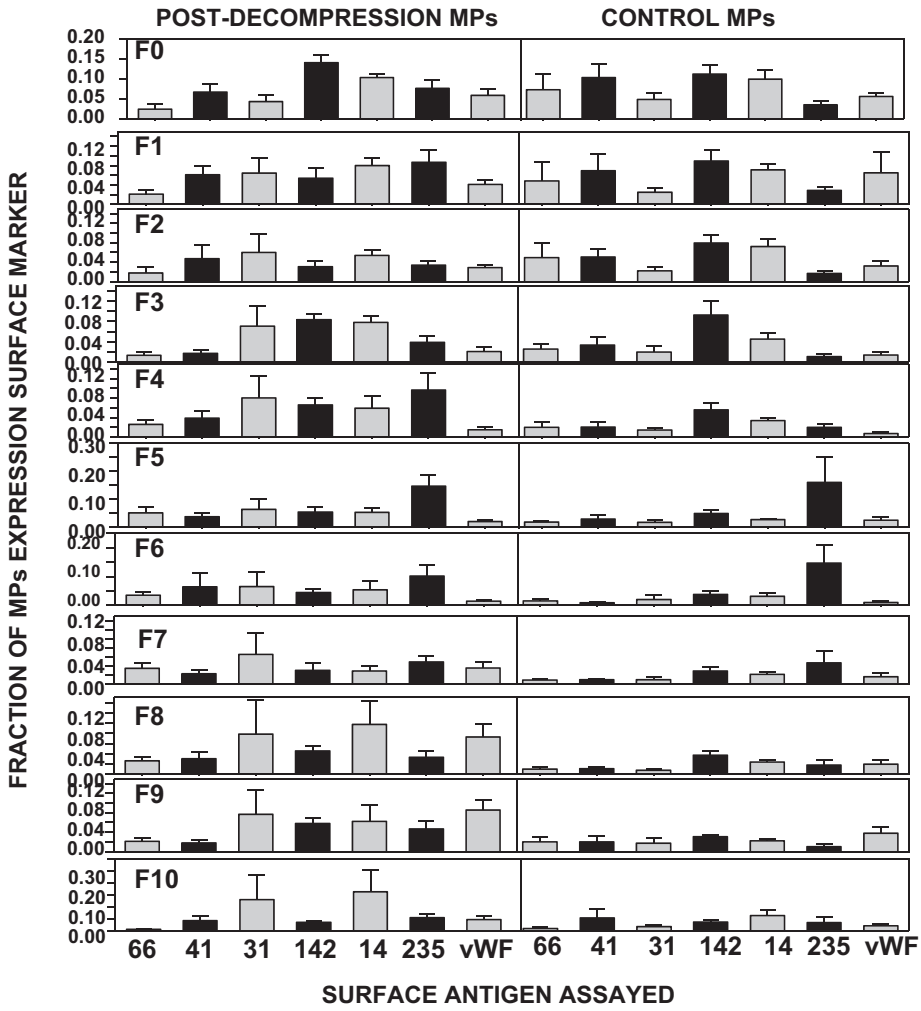

Fig. 2. Survey of microparticle subtypes in the various fractions recovered from sucrose density ultracentrifugation. Data are the fraction of MPs exhibiting the surface markers listed at *bottom*. There were no significant differences in portions of marker expression between decompressed (black bars) and control MP (gray bars) fractions within each sucrose layer (F0 to F10). Density of each layer is shown in Fig. 1.

pressed mouse samples ($n = 4$) exhibited 14.8 ± 5.5% CD63 and 14.5 ± 1.3% Alix-1. Pelleted control mouse samples ($n = 4$) exhibited 6.4 ± 4.1% CD63 and 10.2 ± 2.4% Alix-1, whereas decompressed mouse samples ($n = 4$) exhibited 2.6 ± 4.5% CD63 and 9.3 ± 3.1% Alix-1.

Next, we wanted to assess whether the fraction of buoyant MPs could be altered in samples from normal, control mice by hydrostatic recompression. MP samples were prepared, split in two, and half were subjected to 790-kPa hydrostatic pressure for 1 h. The samples were then suspended in PBS and ultracentrifuged. The fraction of unmanipulated MPs recovered from the PBS surface was 5.00 ± 0.39% and from the middle portion of the PBS column was 9.6 ± 2.0%, and the pellets contained 85.9 ± 2.2% ($n = 4$) of MPs. In MPs that had been subjected to hydrostatic pressure, 3.80 ± 0.14% ($P = 0.039$) were recovered from the PBS surface, 0.03 ± 0.03% ($P = 0.029$) from the middle portion of the PBS column, and 98.9 ± 1.1% ($P = 0.002$) were recovered in the pellets.

NOS isoforms in MPs. Buoyant and pellet MPs were next separated by ultracentrifuging MPs from control mice after suspension in PBS. The two MPs types were lysed and subjected to SDS-PAGE and Western blotting. All three isoforms of nitric oxide synthase (NOS) were present in MPs, but buoyant particles had significantly greater content of type 2 (inflammatory, iNOS) (Fig. 3). Normalized to the actin band from each sample, buoyant particles had 10.7 ± 1.3-fold ($n = 4$, $P < 0.001$) more iNOS than pellet MPs. NOS-1 (neuronal NOS) content was 1.00 ± 0.05 (NS), and NOS-3 (endothelial NOS) was 0.88 ± 0.12-fold (NS) different from pellet MPs.

When MPs from iNOS null (KO) mice were isolated, suspended in PBS, and subjected to ultracentrifugation significantly fewer were in the PBS layer, 1.65 ± 0.05% ($n = 4$, $P < 0.01$) compared with MPs from control mice (5.00 ± 0.39%, as

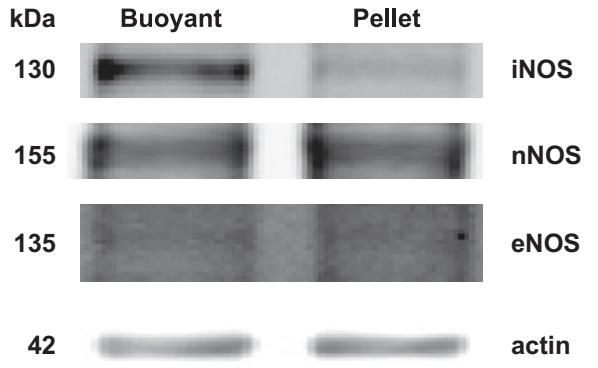

Fig. 3. Representative Western blot showing 3 nitric oxide synthase (NOS) isoforms and actin band in the same preparations of buoyant and pellet MPs. iNOS, inflammatory NOS; nNOS, neuronal NOS; eNOS, endothelial NOS.

discussed above). Moreover, particles from iNOS KO mice were not enlarged after exposure to high-pressure air for 22 h (see Table 1).

Reactive species generation. MPs isolated from control mice were incubated with membrane-permeable fluorophores to evaluate reactive species generated within MPs. Incubation with 4,5-diaminofluorescein diacetate (DAF-DA) exhibited an increase of 0.21 ± 0.02 (SE, $n = 9$) relative fluorescence units (RFU)/min per 1,000 MPs, and incubation with DCF-DA exhibited an increase of 0.40 ± 0.08 RFU/min per 1,000 MPs ($n = 9$). Coincubation with Tiron, a membrane-permeable antioxidant, inhibited fluorescence by 92.5 ± 2.5% ($n = 7$, $P < 0.001$). DAF-DA exhibits greater fluorescence change to reactive nitrogen-derived species (RNS) such as nitric oxide ($^{\cdot}NO$) vs. reactive oxygen species (ROS) and DAF-DA fluorescence was decreased by 43.3 ± 1.4% ($n = 7$, $P < 0.001$) when MPs were preincubated for 30 min with L-NAME, a nonspecific NOS inhibitor, and by 47.6 ± 1.1% ($n = 7$, $P < 0.001$) when preincubated with 1400W, a specific iNOS inhibitor (26).

Cell membranes pose a variable barrier to diffusion of reactive species, including $^{\cdot}NO$ (13, 22). MPs incubated with membrane-impermeant DAF resulted in no fluorescence unless MPs were lysed by adding polyethylene glycol telomere B detergent (PEG) (Fig. 4). PEG was previously shown to lyse MPs (32). If MPs were incubated with L-NAME for 30 min before lysis with PEG, DAF fluorescence was reduced by 49.2 ± 2.9% ($n = 6$, $P < 0.05$) and if lysis was performed in the presence of PTIO, a scavenger of RNS, the fluorescence signal was decreased by 99 ± 1% ($n = 8$, $P < 0.001$) (12).

A similar experiment was next performed using a $^{\cdot}NO$-specific microelectrode. When the electrode was inserted into a MP suspension, no signal registered until PEG was added; but after lysis 0.36 ± 0.05 μM $^{\cdot}NO/1 \times 10^6$ MPs ($n = 5$) was measured. PEG itself caused no signal.

Hypertonic stress or cholesterol removal increase MPs permeability. Radical production was compared between buoyant and pellet MPs from control (no decompression stress) mice separated by ultracentrifugation in PBS. Figure 5*A* shows markedly greater fluorescence following DAF-DA loading in the buoyant vs. pellet MPs and no significant change if these MPs were subjected to an osmotic stress from placement in 0.3 mM mannitol or 2 h pretreatment with 50 mM methyl-β-cyclodextrin (MCD).

We wanted to more closely evaluate the apparently poor diffusion of RNS from within MPs. When buoyant MPs were placed in a solution of DAF the fluorescence increase was negligible unless the solution included 0.3 mM mannitol to cause an osmotic stress (Fig. 5*B*). There was no evidence that mannitol caused MP lysis because fluorescence in the presence of membrane-permeable DAF-DA was not significantly different vs. PBS incubation (Fig. 5*A*) and particle counts were identical before and after the exposure (data not shown).

Incubation with MCD will remove cholesterol from cell membrane lipid bilayers and can alter permeability (16). If buoyant MPs were incubated with 50 mM MCD for 2 h there was a measurable flux of reactive species assessed by DAF. The slope was 10.1 ± 1.9 ($n = 9$) RFU/min per 1×10^5 MPs whereas with incubation in just PBS the slope was −2.2 ± 1.4 ($n = 7$, $P < 0.001$) RFU/min per 1×10^5 MPs (Fig. 5*C*). This was diminished if the MCD-treated MPs were incubated overnight in suspensions containing 750 μM cholesterol, a manipulation shown to reverse some MCD-mediated changes (Fig. 5*D*) (27). The slope of MCD-incubated MPs secondarily incubated with cholesterol was 4.5 ± 1.3 ($n = 7$, $P < 0.02$ vs. 2 h MCD) RFU/min per 1×10^5 MPs, whereas MPs initially incubated with just PBS and then with the cholesterol-containing solution overnight had a slope of −0.9 ± 2.9 ($n = 5$, NS vs. PBS only) RFU/min per 1×10^5 MPs. Fluorescence after DAF-DA loading of these 24 h-incubated MPs did not differ significantly from that shown in Fig. 5*A*, thus indicating no substrate limitation.

Buoyant MPs contain $^{\cdot}NO_2$. We hypothesized that production of RNS may generate nitrogen dioxide ($^{\cdot}NO_2$) within MPs. Interest in $^{\cdot}NO_2$ was prompted because its vapor pressure is ~1 bar (0.1 MPa) at 20°C and almost 2.5 bar at 37°C; thus it may form a gas phase in vivo if diffusion from within MPs was limited. We assayed for $^{\cdot}NO_2$ by placing buoyant MPs in a solution of 100 mM KOH (that causes MPs lysis, data not shown) and 1 mM luminol. Luminescence was 3.2 ± 0.5 ($n = 9$) units/100 MPs, a fluorescence magnitude achieved by adding 1.3 μl of 500 ppm $^{\cdot}NO_2$ gas or 12.5 nM 3-morpholinosydnonimine (SIN-1) to the reaction solution. Luminescence was completely inhibited if suspensions contained Tiron or ebselen, a RNS scavenger. If suspensions contained uric acid, an alternative RNS scavenger, fluorescence was reduced by 70.4 ± 6.8% ($n = 9$, $P < 0.001$). Preincubating MPs with L-NAME decreased luminescence by 27.8 ± 3.5% ($P < 0.001$). When MPs were first subjected to hydrostatic pressure (790 kPa for 1 h) and then assayed, luminescence was reduced 40.0 ± 2.9% ($n = 6$, $P < 0.001$).

Decompression-induced neutrophil activation, vascular leak, and MP elevations after iNOS inhibition or with iNOS KO mice. We next examined whether decompression stress responses differed in WT mice treated with 1400W or in iNOS KO mice. Neutrophil activation was assessed using a flow cytometer (Fig. 6). CD66-expressing cells were gated to select neutrophils, and the magnitude of the CD18 component of β_2 integrins on the surface was quantified as well as surface myeloperoxidase (MPO), which reflects neutrophil degranulation.

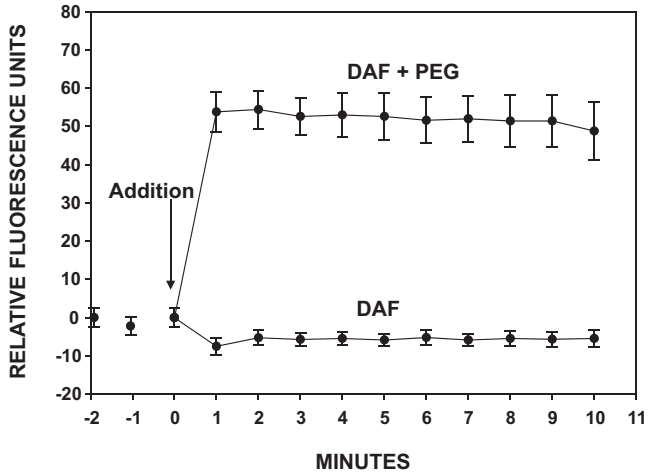

Fig. 4. DAF fluorescence change when MPs are lysed. Figure shows fluorescence using 5 μM DAF in solutions containing 60,000 MPs and impact of adding 0.1% (vol/vol) PEG to lyse MPs. PEG addition without MPs caused no fluorescence signal. Data are means ± SE for 8 experiments.

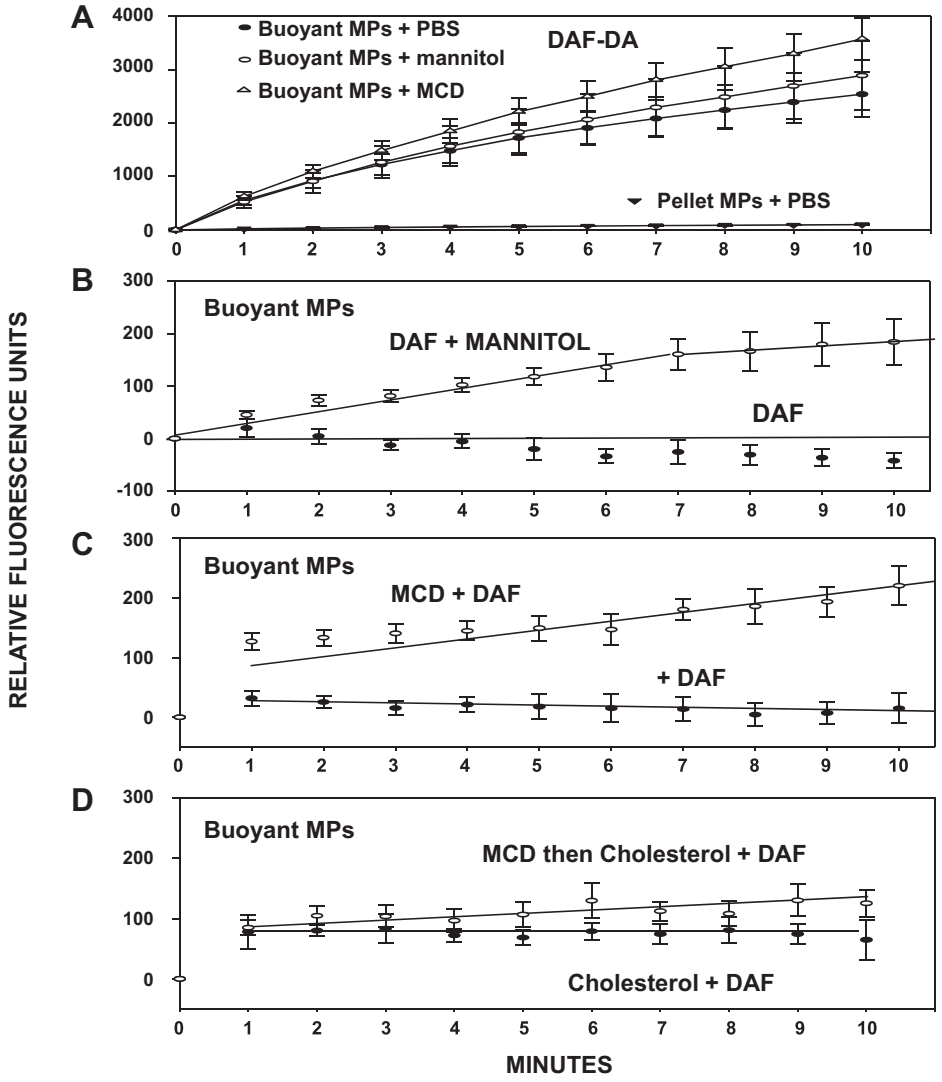

Fig. 5. Fluorescence probes demonstrate reactive species production by MPs. *A*: fluorescence using membrane-permeable DAF-DA with buoyant or pellet MPs incubated with PBS, 0.3 mM mannitol, or 50 mM methyl-β-cyclodextrin (MCD). *B*: membrane impermeant DAF fluorescence when buoyant MPs are incubated without or with 0.3 mM mannitol. Regression lines are shown. *C*: DAF fluorescence when buoyant MPs are first incubated with MCD for 2 h. *D*: DAF fluorescence after buoyant MPs were incubated with MCD for 2 h, then overnight with 750 μM cholesterol. Note that with MCD experiments regression lines do not extend to the origin. Fluorescence was 0 at initiation of the trials, MPs were added and the 1 min reading was the first taken after MPs addition. Data show fluorescence (relative units) with 2×10^5 MPs in each preparation and are all means ± SE for 4–12 independent experiments.

Expression of the platelet-specific protein CD41 on neutrophils was also evaluated as an index of platelet-neutrophil interactions, which are elevated after decompression stress (32, 41). Based on all three parameters, there was significantly less decompression-induced neutrophil activation with 1400W treatment and in iNOS KO mice.

Postdecompression vascular injury was quantified by assessing leakage of lysine fixable rhodamine-dextran (2×10^6 Da). As in previous studies, multiple organs were surveyed because of varied patterns of postdecompression injuries (11, 35). Capillary leak was significantly less in all organs of decompressed WT mice treated with 1400W and in all organs except brain of decompressed iNOS KO mice (Fig. 7*A*). Consistent with prior studies, there were significantly more circulating MPs in mice 1 h after exposure to 790 kPa air pressure for 2 h (32, 41). Whereas control mice had 2,085 ± 37 MPs/μl plasma ($n = 20$), decompressed mice had 8,079 ± 105 ($n = 24$, $P < 0.001$) MPs/μl plasma. Control KO mice had 2,222 ± 209 MPs/μl plasma ($n = 20$, NS vs. WT) and decompressed KO mice had 2,005 ± 131 MPs/μl plasma ($n = 13$, NS). At 3 h after 1400W, treatment normal, air-breathing WT mice had only 381 ± 41 MPs/ μl plasma($n = 4$, $P < 0.05$ vs. WT mice), and those injected with 1400W, exposed to 790 kPa air pressure for 2 h, and studied 1 h later (3 h postinjection) had 510 ± 32 ($n = 4$, NS vs. ambient air-exposed, 1400W-treated mice). Surface expression of antigens on MPs in these various groups of mice exhibited a complex pattern that was not discernibly different (data not shown).

MPs injection into naïve mice. One possible explanation for why inflammatory events did not occur in 1400W-treated and KO mice was that there was no increase in circulating MPs postdecompression. Therefore, MPs from decompressed WT and KO mice were prepared and 1.27×10^6 MPs injected into naïve mice following our published techniques (41). As shown in Fig. 6, compared with control mice injected with just PBS, injection of MPs from KO mice did not elicit the same magnitude of neutrophil activation as did WT MPs. Similarly, vascular leak differed significantly between mice injected with WT vs. KO MPs (Fig. 7*B*).

DISCUSSION

Results from this study indicate that ~5% of circulating MPs in normal, control mice are buoyant in saline and ~8%

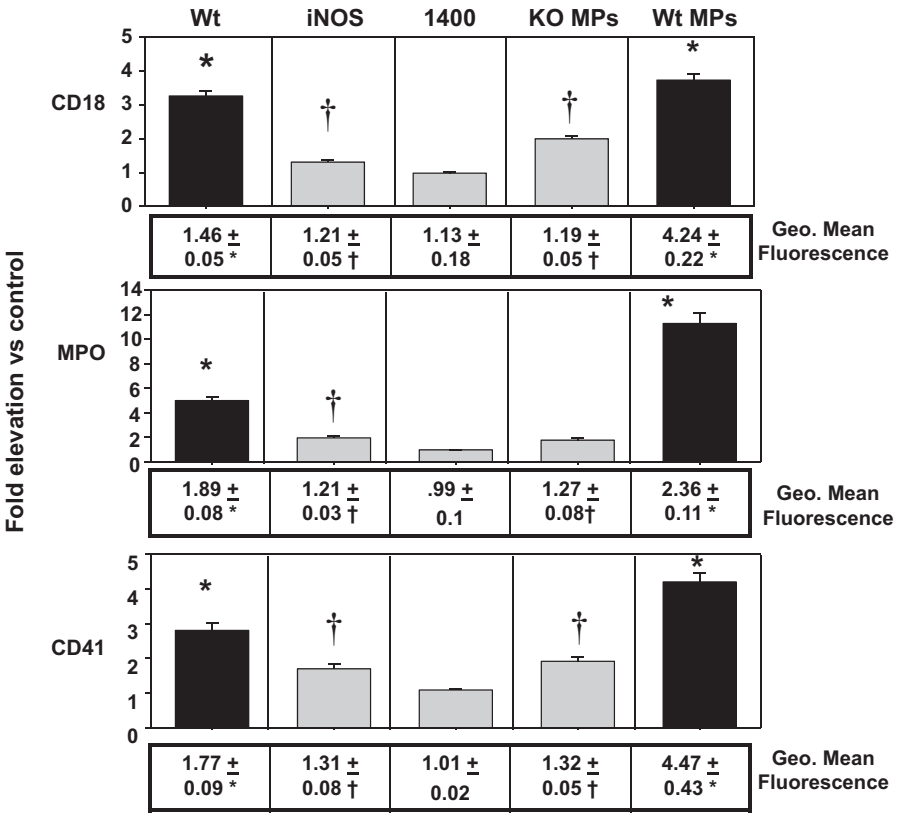

Fig. 6. Neutrophil activation after decompression stress or injection of MPs from decompressed mice. Bar graphs show fold elevation in fraction of neutrophils that express CD18, MPO, and CD41 with mean fluorescence above 10 arbitrary units. The fold increase in geometric mean fluorescence in each sample type is shown in the numbers beneath bar graphs. WT indicates fold elevation compared with wild-type control, air-breathing mice. The iNOS label shows fold elevation in iNOS knockout (KO) mice subjected to decompression relative to fraction of neutrophils in control iNOS KO mice. The label 1400 indicates fold-elevation from decompressed wild-type mice vs. control mice injected ip with 25 mg/kg 1400W 3 h earlier (immediately before exposure to air pressure in the decompression group). Rightmost two bar graphs show increase in surface expression when mice are injected with either 1.27×10^6 MPs from decompressed iNOS KO or WT mice compared against mice injected with only PBS. Data are means ± SE; $n = 4$–9 independent experiments. *$P < 0.05$ vs. control, †$P < 0.05$ vs. control and WT groups.

possess a gas phase because they enlarge with decompression following ex vivo exposure to high-pressure air (Table 1). Consistent with this view, the fraction of buoyant MPs from control mice could be reduced by hydrostatic recompression. These data provide the first characterization of what can serve as a cavitation nucleus to form bubbles in vivo.

We analyzed MPs several ways. Using sucrose gradient centrifugation we found a significant difference from control only with the least dense MPs fraction from decompressed mice (Fig. 1). There were no significant differences in surface markers among the MPs with different densities from control and decompressed mice (Fig. 2). Characterization with this

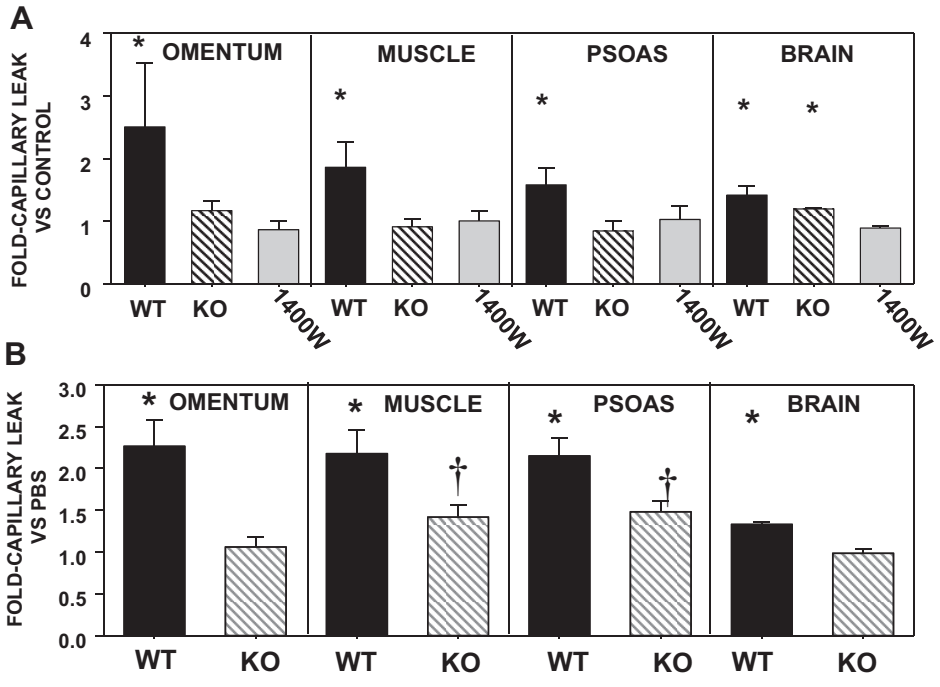

Fig. 7. Vascular leak associated with decompression stress. Tissues were prepared and evaluated as described in METHODS AND MATERIALS to assess leakage of lysine-fixable Rhodamine-conjugated 2×10^6 Da dextran. Values reflect the ratio of fluorescence/mg protein in homogenates from injected decompressed mice vs. fluorescence in homogenates from control mice injected with the same lot of Rhodamine-dextran and run on the same day. *A*: vascular leak in various tissues of WT mice, those injected with 1400W, and iNOS KO mice. *B*: vascular leak in mice injected with either 1.27×10^6 MPs from decompressed iNOS KO or WT mice compared against mice injected with only PBS. Values are means ± SE; $n = 4$–6 for each group, *$P <$ 0.05 vs. control, †$P < 0.05$ vs. control and WT groups.

approach appears to have limited analytical value, however, because there is a dynamic sharing of surface markers once MPs form (32, 41). Because of this promiscuous exchange, we cannot reliably assess whether a portion of MPs in our study are derived from exosomes.

We also evaluated some biochemical characteristics of MPs, having reasoned that gas formation de novo in MPs would likely arise from intrinsic metabolic activity. Buoyant particles are enriched 10-fold in iNOS (Fig. 3). This enzyme appears to be the gas source because there is a smaller fraction of buoyant MPs in iNOS KO mice, and ex vivo air pressure does not cause these MPs to enlarge. Given the rapid catalytic rate of iNOS vs. other NOS isoforms, as well as its tendency to produce both $^{\cdot}NO$ and superoxide ($O_2^{\cdot-}$), a wide variety of reactive species will be generated MPs (33).

Using a relatively specific assay, buoyant MPs appear to contain $^{\cdot}NO_2$. The propensity of $^{\cdot}NO_2$ to form a gas phase would in part relate to its vapor pressure and to some chemical peculiarities. In contrast to many reactive species such as $^{\cdot}NO$, $ONOO^-$, and $ONOOCO_2^-$, $^{\cdot}NO_2$ is not hydrolyzed in aqueous medium; its degradation in water only occurs after it reacts with $^{\cdot}NO$ to form N_2O_3 or diverges to N_2O_4 (33). Separate from these chemical attributes, gas formation would also require a limitation to diffusion out of MPs. Conventional wisdom is that RNS readily diffuse through lipid membranes. Experimental data with $^{\cdot}NO_2$ is quite sparse, although its membrane permeability has been estimated to be relatively rapid based on solubility modeling (28). Evidence in this study indicates, however, that $^{\cdot}NO_2$ has limited permeability through the buoyant MPs membranes (Figs. 4 and 5). Assuming that all $^{\cdot}NO_2$ reacted with luminol in the assay when MPs were lysed, there are $\sim 1.7 \times 10^{11}$ molecules of $^{\cdot}NO_2$ per MP. Therefore, most $^{\cdot}NO_2$ must be dissolved as this would represent a volume of 6.5×10^3 μm^3. Consistent with this view, luminescence was reduced by only about one-quarter when buoyant MPs were subjected to hydrostatic recompression before the assay.

With regard to the pathological implications of gas-containing MPs in decompression stress, the central role for iNOS was shown by studies with a chemical inhibitor, 1400W, as well as iNOS KO mice. Inhibition of iNOS virtually eliminates postdecompression neutrophil activation and capillary leak (Figs. 6 and 7). Neutrophil activation was less in decompressed KO mice vs. WT mice. Neutrophil activation still occurred in KO mice, however, which may relate to one or more compensatory changes. For example, alternative NOS isoforms may have increased as data show that MPs contain all three types. The presence of capillary damage in the brains of decompressed iNOS KO mice may be due to persistent neutrophil activation.

The critical role played by iNOS in decompression stress was most convincingly demonstrated by injecting MPs into naïve mice. When equal numbers were injected, inflammatory changes were markedly less with MPs obtained from decompressed KO mice vs. WT mice. Additionally, KO mice and WT mice treated with 1400W did not exhibit elevations in circulating MPs that normally occur due to decompression stress. Surprisingly, 1400W resulted in a marked reduction of MPs compared with normal WT mice.

There is a body of work in animals suggesting a role for $^{\cdot}NO$ in the formation of vascular bubbles as well as pathophysiological responses to their presence (6, 23, 34, 39, 40). Infusing $^{\cdot}NO$ donor drugs reduces injury in decompressed animals and decreases the number of intravascular bubbles in both animals and humans (6, 23, 34, 39). Given the varied effects of $^{\cdot}NO$ these findings are not necessarily contradictory to observations in our study. That is, $^{\cdot}NO$ donors can alter blood flow and also leukocyte-endothelial cell adherence which may be beneficial once bubbles have already been formed. Inhibiting $^{\cdot}NO$ synthesis using a nonspecific NOS inhibitor increases lethality of severe decompression stress in sedentary but not exercised rats (40). This could arise due to greater cardiovascular effects with this agent vs. a selective iNOS inhibitor such as 1400W, or due to some other secondary process such as enhancing neutrophil MPs formation (24).

In prior studies, we showed that increases in the number and size of MPs associated with decompression trigger platelet-neutrophil interactions and neutrophil activation, and vascular damage follows these events (31, 41). An obvious question from these and the present results is why should enlarged MPs trigger neutrophil activation? One possibility is that, based on latest findings, MPs serve to initiate bubble growth and once formed, it is the bubbles that cause widespread physical damage. Thus postdecompression removal of MPs by systemic administration of polyethylene glycol telomere B or anti-annexin antibodies abates vascular injuries because fewer bubbles are formed (31). The process could also be much more complex, however, because it may be possible that internalization of $^{\cdot}NO_2$-containing particles, in particular, initiates cell activation. The major MP clearance pathway is thought to involve lactadherin binding to surface-expressed phosphatidylserine and subsequent clearance via splenic macrophages (4). This would likely limit systemic vascular inflammatory responses. Recently, however, an alternative pathway involving MPs binding by Del-1 on endothelial cells opens the way for a systemwide trafficking of MPs that, if delivering a potential toxin such as $^{\cdot}NO_2$, could participate in tissue injury (5).

RNS play roles in cell signaling as well as oxidative and nitrosative stress (33). Production of RNS by MPs has intriguing physiological implications and they may play varied roles in transcirculatory signaling. The marked reduction of MPs in mice treated with 1400W and absence of elevations in decompressed iNOS KO mice implicates RNS play a role in MP generation and possibly in MP clearance. These issues require further investigation. Finally, showing that iNOS metabolism with $^{\cdot}NO_2$ generation results in a gas nucleation site within MPs opens the way for further research into novel ways one might abrogate the risk of provocative decompression.

ACKNOWLEDGMENTS

We acknowledge very helpful discussions with Drs. W. Boron and Robert Geyer.

GRANTS

Funding was provided by a grant from the Office of Naval Research.

DISCLOSURES

No conflicts of interest, financial or otherwise, are declared by the author(s).

AUTHOR CONTRIBUTIONS

Author contributions: S.R.T. conception and design of research; S.R.T., M.Y., V.M.B., T.N.M., M.B., and D.G.B. performed experiments; S.R.T., M.Y., and D.G.B. analyzed data; S.R.T. interpreted results of experiments; S.R.T. prepared figures; S.R.T. drafted manuscript; S.R.T. and D.G.B. edited

and revised manuscript; S.R.T., M.Y., V.M.B., T.N.M., M.B., and D.G.B. approved final version of manuscript.

REFERENCES

1. **Buerk DG, Riva CE, Cranstoun SD.** Nitric oxide has a vasodilatory role in cat optic nerve head during flicker stimuli. *Microvasc Res* 52: 13–26, 1996.
2. **Connor DE, Exner T, Ma DD, Joseph JE.** The majority of circulating platelet-derived microparticles fail to bind annexin V, lack phospholipid-dependent procoagulant activity and demonstrate greater expression of glycoprotein Ib. *Thromb Haemost* 103: 1044–1052, 2010.
3. **Daniels S, Eastaugh KC, Paton WDM, Smith EB.** Micronuclei and bubble formation: a quantitative study using the common shrimp, *Crangon crangon*. In: *Underwater Physiology VIII: Proceedings of the Eighth Symposium on Underwater Physiology,* edited by Bachrach AJ, Matzen MM. Bethesda, MD: Undersea Medical Society, 1984, p. 147–157, 1984.
4. **Dasgupta SK, Abdel-Monem H, Niravath P, Le A, Bellera RV, Langlois K, Nagata S, Rumbaut RE, Thiagarajan P.** Lactadherin and clearance of platelet-derived microvesicles. *Blood* 113: 1332–1339, 2009.
5. **Dasgupta SK, Le A, Chavakis T, Rumbaut RE, Thiagarajan P.** Developmental endothelial locus-1 (Del-1) mediates clearance of platelet microparticles by the endothelium. *Circulation* 125: 1664–1672, 2012.
6. **Dujic Z, Palada I, Valic Z, Duplancic D, Obad A, Wisloff U, Brubakk AO.** Exogenous nitric oxide and bubble formation in divers. *Med Sci Sports Exerc* 38: 1432–1435, 2006.
7. **Eftedal OS, Lydersen S, Brubakk AO.** The relationship between venous gas bubbles and adverse effects of decompression after air dives. *Undersea Hyperb Med* 34: 99–105, 2007.
8. **Enjeti AK, Lincz LF, Seldon M.** Detection and measurement of microparticles: an evolving research tool for vascular biology. *Semin Thromb Hemost* 33: 771–779, 2007.
9. **Enjeti AK, Lincz LF, Seldon M.** Microparticles in health and disease. *Semin Thromb Hemost* 34: 683–692, 2008.
10. **Fox FE, Herzfeld KF.** Gas bubbles with organic skins as cavitation nuclei. *J Acoust Soc Am* 26: 984–989, 1954.
11. **Francis TJ, Pearson RR, Robertson AG, Hodgson M, Dutka AJ, Flynn ET.** Central nervous system decompression sickness: latency of 1070 human cases. *Undersea Hyperb Med* 15: 404–417, 1988.
12. **Goldstein S, Russo A, Samuni A.** Reactions of PTIO and carboxy-PTIO with nitric oxide, nitrogen dioxide and superoxide. *J Biol Chem* 278: 50949–50955, 2003.
13. **Herrera M, Hong NJ, Garvin JL.** Aquaporin-1 transports NO across cell membranes. *Hypertension* 48: 157–164, 2006.
14. **Hugel B, Martinez MC, Kunzelmann C, Freyssinet JM.** Membrane microparticles: Two sides of the coin. *Physiology* 20: 22–27, 2005.
15. **Jy W, Mao WW, Horstman L, Tao J, Ahn YS.** Platelet nicroparticles bind, activate and aggregate neutrophils in vitro. *Blood Cell Mol Dis* 21: 217–231, 1995.
16. **Klein U, Gimpl G, Fahrenholz F.** Alteration of the myometrial plasma membrane cholesterol content with beta-cyclodextrin modulates the binding affinity of the oxytocin receptor. *Biochemistry* 34: 13784–13793, 1995.
17. **Lo SC, Hung CH, Lin DT, Peng HC, Huang TF.** Involvement of platelet glycoprotein Ib in platelet nicroparticle mediated neutrophil activation. *J Biomed Sci* 13: 787–796, 2006.
18. **Madden LA, Chrismas BC, Mellor D, Vince RV, Midgley AW, McNaughton LR, Atkins SL, Laden G.** Endothelial function and stress response after simulated dives to 18 msw breathing air or oxygen. *Aviat Space Environ Med* 81: 41–51, 2010.
19. **Mause SF, Weber C.** Microparticles: Protagonists of a novel communication network for intercellular information exchange. *Circ Res* 107: 1047–1057, 2010.
20. **McDonough PM, Hemmingsen EA.** Bubble formation in crabs induced by limb motions after decompression. *J Appl Physiol* 57: 117–122.
21. **Mesri M, Altieru DC.** Leukocyte microparticles stimulate endothelial cell cytokine release and tissue factor induction in a JNK1 signaling pathway. *J Biol Chem* 274: 23111–23118, 1999.
22. **Moller MN, Lancaster JR Jr, Denicola A.** The interaction of reactive oxygen and nitrogen species with membranes. In: *Current Topics in Membranes 61. Free Radical Effects on Membranes,* edited by Matalon S, New York: Academic, 2008, p. 23–43.
23. **Mollerlokken A, Berge VJ, Jorgensen A, Wisloff U, Brubakk AO.** Effect of a short-acting NO donor on bubble formation from a saturation dive in pigs. *J Appl Physiol* 101: 1541–1545, 2006.
24. **Nolan S, Dixon R, Norman K, Hellewell PG, Ridger V.** Nitric oxide regulates neutrophil migration through microparticle formation. *Am J Pathol* 172: 265–273, 2008.
25. **Pirro M, Schillaci G, Bagaglia F, Menecali C, Paltriccia R, Mannarino MR, Capanni M, Velardi A, Mannarino E.** Microparticles derived from endothelial progenitor cells in patients at different cardiovascular risk. *Atherosclerosis* 197: 757–767, 2008.
26. **Price M, Kessel D.** On the use of fluorescence probes for detecting reactive oxygen and nitrogen species associated with photodynamic therapy. *J Biomedical Optics* 15: 051605–051601-051603, 2010.
27. **Rodal SK, Skretting G, Garred O, Vilhardt F, van Deurs B, Sandvig K.** Extraction of cholesterol with methyl-beta-cyclodextrin perturbs formation of clathrin-coated endocytic vesicles. *Mol Biol Cell* 10: 961–974, 1999.
28. **Santiago S, Moller MN, Coitino EL, Denicola A.** Nitrogen dioxide solubility and permeation in lipid membranes. *Arch Biochem Biophys* 512: 190–196, 2011.
29. **Thery C, Clayton A, Amigorena S, Raposo G.** Isolation and characterization of exosomes from cell culture supernatants and biological fluids. *Curr Protocols Cell Biol Suppl* 30: 3.33.31–33.22.29, 2006.
30. **Thom SR, Bhopale V, Fisher D, Manevich Y, Huang PL, Buerk DG.** Stimulation of nitric oxide synthase in cerebral cortex due to elevated partial pressures of oxygen: an oxidative stress response. *J Neurobiol* 51: 85–100, 2002.
31. **Thom SR, Milovanova TN, Bogush M, Bhopale VM, Yang M, Bushmann K, Pollock NW, Ljubkovic M, Dujic Z.** Microparticle production, neutrophil activation and intravascular bubbles following open-water SCUBA diving. *J Appl Physiol* 112: 1268–1278, 2012.
32. **Thom SR, Yang M, Bhopale VM, Huang S, Milovanova TN.** Microparticles initiate decompression-induced neutrophil activation and subsequent vascular injuries. *J Appl Physiol* 110: 340–351, 2011.
33. **Thomas DD, Ridnour LA, Isenberg JS, Flores-Santana W, Switzer CH, Sonzelli S, Hussain P, Vecoli C, Paolocci N, Ambs S, Colton CA, Harris CC, Roberts DD, Wink DA.** The chemical biology of nitric oxide: Implications in cellular signaling. *Free Radic Biol Med* 45: 18–31, 2008.
34. **Valic Z, Palada I, Dujic Z.** Short-acting NO donor and decompression sickness in humans. *J Appl Physiol* 102: 1541–1545, 2007.
35. **Vann RD.** Mechanisms and risk of decompression. In: *Bove and Davis' Diving Medicine* (4th ed.), edited by Bove AA. Philadelphia, PA: Saunders, 2004, p. 127–183.
36. **Vann RD, Grimstad J, Nielsen CH.** Evidence for gas nuclei in decompressed rats. *Undersea Hyperb Med* 7: 107–112, 1980.
37. **Vince RV, McNaughton LR, Taylor L, Midgley AW, Laden G, Madden LA.** Release of VCAM-1 associated endothelial microparticles following simulated SCUBA dives. *Eur J Appl Physiol* 105: 507–513, 2009.
38. **Wendel GJ, Stedman DH, Cantrell CA.** Luminol-based nitrogen dioxide detector. *Anal Chem* 55: 937–940, 1983.
39. **Wisloff U, Richardson RS, Brubakk AO.** Exercise and nitric oxide prevent bubble formation: a novel approach to the prevention of decompression sickness? *J Physiol* 555: 825–829, 2004.
40. **Wisloff U, Richardson RS, Brubakk AO.** NOS inhibition increases bubble formation and reduces survival in sedentary but not exercised rats. *J Physiol* 546: 577–582, 2003.
41. **Yang M, Milovanova TN, Bogush M, Uzan G, Bhopale VM, Thom SR.** Microparticle enlargement and altered surface proteins after air decompression are associated with inflammatory vascular injuries. *J Appl Physiol* 112: 204–211, 2012.
42. **Yount DE.** On the elastic properties of the interfaces that stabilize gas cavitation nuclei. *J Colloid Interface Sci* 193: 50–59, 1997.
43. **Yount DE, Kunkle TD, D'Arrigo JS.** Stabilization of gas cavitation nuclei by surface active compounds. *Aviat Space Environ Med* 48: 185–189, 1977.